Genetic Alterations in Mouse Medulloblastomas and Generation of Tumors *De novo* from Primary Cerebellar Granule Neuron Precursors

Frederique Zindy,[1] Tamar Uziel,[1] Olivier Ayrault,[1] Christopher Calabrese,[2] Marc Valentine,[1] Jerold E. Rehg,[3] Richard J. Gilbertson,[2] Charles J. Sherr,[1,4] and Martine F. Roussel[1]

Departments of [1]Genetics and Tumor Cell Biology, [2]Developmental Neurobiology, and [3]Pathology and [4]Howard Hughes Medical Institute, St. Jude Children's Research Hospital, Memphis, Tennessee

Abstract

Mice lacking *p53* and one or two alleles of the cyclin D–dependent kinase inhibitor $p18^{Ink4c}$ are prone to medulloblastoma development. The tumor frequency is increased by exposing postnatal animals to ionizing radiation at a time when their cerebella are developing. In irradiated mice engineered to express a floxed *p53* allele and a *Nestin-Cre* transgene, tumor development can be restricted to the brain. Analysis of these animals indicated that inactivation of one or both *Ink4c* alleles did not affect the time of medulloblastoma onset but increased tumor invasiveness. All such tumors exhibited complete loss of function of the *Patched 1* (*Ptc1*) gene encoding the receptor for sonic hedgehog, and many exhibited other recurrent genetic alterations, including trisomy of chromosome 6, amplification of N-*Myc*, modest increases in copy number of the *Ccnd1* gene encoding cyclin D1, and other complex chromosomal rearrangements. In contrast, medulloblastomas arising in $Ptc1^{+/-}$ mice lacking one or both *Ink4c* alleles retained p53 function and exhibited only limited genomic instability. Nonetheless, complete inactivation of the wild-type *Ptc1* allele was a universal event, and trisomy of chromosome 6 was again frequent. The enforced expression of N-Myc or cyclin D1 in primary cerebellar granule neuron precursors isolated from $Ink4c^{-/-}$, $p53^{-/-}$ mice enabled the cells to initiate medulloblastomas when injected back into the brains of immunocompromised recipient animals. These "engineered" tumors exhibited gene expression profiles indistinguishable from those of medulloblastomas that arose spontaneously. These results underscore the functional interplay between a network of specific genes that recurrently contribute to medulloblastoma formation. [Cancer Res 2007;67(6):2676–84]

Introduction

Medulloblastoma and supratentorial primitive neuroectodermal tumors are the most common malignant brain tumors in children. Although modern therapeutic protocols cure >60% of such children, the survivors' quality of life is usually severely compromised due to adverse effects of therapy on neurocognitive functions. Human medulloblastomas can be classified into multiple histologic variants (1), including the large cell anaplastic type that is thought to be the least curable (2). Through a combination of molecular techniques, several genes encoding proteins that act within developmental signaling pathways have been implicated in medulloblastoma development, and the contributions of some have been tested in mouse models of the disease. Alterations of genes in the sonic hedgehog (*SHH*)/*PATCHED* (*PTC1*) signaling pathway as well as mutations in *β-CATENIN* and *NOTCH* genes play roles in human medulloblastoma (3–7). In most mouse models, inactivation of *p53* is a prerequisite for medulloblastoma development, whereas, in humans, *TP53* mutations are infrequent and do not correlate with specific aberrations in Ptc, Notch, or β-catenin signaling (8).

During mouse development, cerebellar granule neuron progenitors (CGNPs) rapidly divide in the external granule layer (EGL) from postnatal day (P) 1 to P7, after which they exit the cell cycle and migrate inward through the Purkinje cell layer to form the internal granule layer (IGL). The latter zone is composed uniquely of postmitotic cells that extend retrograde neurites that synapse to Purkinje cell dendrites within the molecular layer of the mature organ (9, 10). This entire process is terminated by P21. It is thought that a subset of medulloblastomas originates from CGNPs that fail to exit the cycle and migrate, thus yielding tumor cells that mainly arise at the cerebellar periphery (11, 12).

The *Ink4c* gene, which encodes a polypeptide inhibitor ($p18^{Ink4c}$) of the cyclin-dependent kinases (Cdk), Cdk4 and Cdk6, is induced transiently in CGNPs before their exit from the cell cycle (13), but the protein persists throughout subsequent phases of cerebellar patterning.[5] Although loss of *Ink4c* alone is insufficient to trigger tumorigenesis in the mouse cerebellum, its inactivation collaborates with *p53* loss, or independently, with disruption of one *Ptc1* allele, to generate medulloblastoma in mice (13, 14). Mice lacking both *Ink4c* and *p53* develop medulloblastoma with low penetrance (14), but the incidence increases to 75% within 6 months when mice are irradiated at P7 (13). *Ptc1* heterozygous mice that lack either one or two *Ink4c* alleles develop medulloblastoma with ~50% incidence, also within 6 months of birth (13). The incomplete frequency of tumor formation in both mouse medulloblastoma models and the accelerating effects of ionizing radiation in $Ink4c^{-/-}$, $p53^{-/-}$ mice imply that additional genetic events contribute to tumor formation.

To better understand the spectrum of chromosomal alterations associated with these two mouse models, we have further analyzed the emerging medulloblastomas by use of spectral karyotyping

Note: Supplementary data for this article are available at Cancer Research Online (http://cancerres.aacrjournals.org/).

F. Zindy and T. Uziel contributed equally to this work.

Requests for reprints: Martine F. Roussel, Department of Genetics and Tumor Cell Biology, St. Jude Children's Research Hospital, 332 North Lauderdale, Memphis, TN 38105. Phone: 901-495-3481; Fax: 901-495-2381; E-mail: martine.roussel@stjude.org.

doi:10.1158/0008-5472.CAN-06-3418

[5] O. Ayrault and M.F. Roussel, unpublished data.

(SKY), fluorescence *in situ* hybridization (FISH), and array comparative genomic hybridization (CGH). Recurrent genetic alterations were identified that were either common to both mouse models of medulloblastoma or specific to one or the other. To further test the importance of these genetic events in accelerating tumor development, we introduced particular genes into purified, primary CGNPs explanted from tumor-prone mice and injected the modified cells into immunocompromised recipient animals. Our results underscore functional interactions between a group of specific genes that have also been implicated in human medulloblastoma development.

Materials and Methods

Animal husbandry. Breeding and genotyping of mice were done as reported previously (13). Where indicated, mice were irradiated at P7 using a cesium source delivering 4 Gy. Mice were housed in an American Association of Laboratory Animal Care–accredited facility in accordance with NIH Guidelines.

Spectral karyotyping. SKY was done as recommended by the manufacturer using the Applied Spectral Imaging (ASI, Vista, CA) SkyPaint kit for mouse chromosomes. Images were acquired with a fluorescence microscope equipped with an interferometer (Spectra Cube TM, ASI) and custom designed filter cube (Chroma Technologies, Rockingham, VT) and analyzed using SKY View version 2.1 software (ASI).

FISH analysis. Purified DNA from bacterial artificial chromosome (BAC) clones was labeled by nick translation using either digoxigenin dUTP or biotin dUTP. Labeled DNA was mixed with sheared genomic DNA and resuspended in buffer [50% formamide, 10% dextran sulfate, 2× SSC (1× SSC is 0.15 mol/L NaCl, 0.015 mol/L sodium citrate)]. The probe was denatured in water at 70°C for 5 min. Slides were immersed in 70% formamide and 2× SSC at 70°C for 2 min. After overnight hybridization at 37°C, unbound probe was removed in 50% formamide and 2× SSC at 37°C for 4 min. Signals were detected with anti-digoxigenin FITC or Texas red avidin. Slides were counterstained using 4′,6-diamidino-2-phenylindole.

Array CGH. Genomic arrays containing 6,528 mouse BAC clones (Roswell Park Cancer Institute Microarray Facility) generated by ligation-mediated PCR (15) were printed in triplicate on amino-silanated glass slides (Schott Nexterion type A+) using 10K Microspot pins and a MicroGrid II TAS arrayer (BioRobotics, Ann Harbor, MI). Undigested genomic DNA was labeled and hybridized according to basic Protocol 4 (16) except that hybridizations and washes were done manually using a BioArray labeling system (Enzo, Farmingdale, NY) and mouse Cot1 DNA (Invitrogen, Carlsbad, CA). Images acquired with a Genepix 4000B scanner were analyzed with GenePix 6.0 software (Axon Corp., Union City, CA). For spots having signal-to-noise ratio >2.5 in at least one channel, the ratio was calculated from the background-subtracted median signal of the two channels. To remove intensity-specific bias, ratios were normalized on log scale with a nonlinear algorithm by applying print tip Loess function (17) using the R language–based Bioconductor[6] (release 1.9). Results of triplicate replicas were combined by taking the mean of log ratios. Any BAC that had less than two replicates passing quality control steps was excluded. BAC clone mapping information[7] (August 2005 mouse Build 35) was added to the resulting ratios. The final ratio represents the relative copy number of DNA from the experimental sample and the reference control sample.

Histopathology and immunohistochemistry. Mice exhibiting signs of illness (abnormal head movements, cranial expansion, scruffy hair, reduced activity, or ataxia) were sacrificed, and recovered tumors were fixed in 10% neutral-buffered formalin, embedded in paraffin, sectioned at 4 μm, stained with H&E, and examined microscopically (14). Immunohistochemistry of medulloblastomas was done (14) using antibodies to class III β-tubulin (TUJ1; 1:1,000; Covance, Berkeley, CA), synaptophysin (1:100) and glial fibrillary acidic protein (GFAP; 1:500; both from DAKO, Carpinteria, CA), green fluorescent protein (GFP; 1:200; Molecular Probes, Eugene, OR), and cyclin D1 (1:100; Santa Cruz Biotechnology, Santa Cruz, CA). Medulloblastomas were defined by anatomic location, tumor cell morphology, and expression of specific neural proteins revealed by immunohistochemistry.

Immunoblotting. Cerebella, medulloblastoma samples, or purified tumor cells were homogenized in lysis buffer [50 mmol/L HEPES (pH 7.5), 150 mmol/L NaCl, 1 mmol/L EDTA, 2.5 mmol/L EGTA, 0.1% Tween 20, 0.1% SDS, containing protease inhibitors], sonicated twice for 5 s, left on ice for 30 min, and centrifuged to remove debris. Proteins (20 μg/lane) were loaded onto SDS polyacrylamide gels (NuPAGE, Invitrogen) and transferred to Immobilon-P membranes (Millipore, Bedford, MA). Membranes were saturated with 5% milk/TBS-Tween 20 and incubated in 5% milk/TBS-Tween 20 containing the following antibodies at 1:500 dilution: anti-cyclin D1 (72-13G), anti-cyclin D2 (34B1-3), anti-Cdk2 (M2), anti-Cdk4 (C-22), anti-Cdk6 (C-21), anti-actin (C-11; all from Santa Cruz Biotechnology), anti–N-Myc mouse monoclonal antibody (NCM II 100; Calbiochem, Temecula, CA), anti–phospho-Akt 473 (Cell Signaling Technology, Danvers, MA), and anti-Pten (RB-072-P1, Neomarkers, Fremont, CA). After washes in TBS-Tween 20, secondary antibodies coupled with peroxidase (Amersham, Little Chalfort, United Kingdom) were used to detect signals by enhanced chemiluminescence (Perkin-Elmer, Boston, MA).

CGNP purification and retroviral infection. Purification of CGNPs from mouse cerebella (18) and proliferation studies were done as described (13). Percoll-purified CGNPs were infected during the preplating stage with murine stem cell virus–based retroviruses, either as empty vectors carrying only GFP expressed from an internal ribosomal entry site or also carrying N-*Myc* or *cyclin D1* cDNAs. Infected CGNPs were injected into mice (see below) without prior cell culture.

Orthotopic injections. Female CD-1 *nu/nu* mice (Charles River Laboratories, Wilmington, MA) ages 8 to 12 weeks were anesthetized and placed into a stereotactic apparatus equipped with a *Z*-axis (Kopf Instruments, Tujunga, CA). A portion of the scalp was removed, a window (approximately 10 × 5 mm) was made in the skull using a dental drill, and the pia was excised. Infected CGNPs (2×10^6 to 3×10^6 cells) resuspended in Matrigel (5 μL; BD BioSciences, Bedford, MA) were implanted into the cerebrum at a depth of 0.5 to 2 mm using a 25 μL Hamilton syringe with an unbeveled 30-gauge needle. The wound was covered with a sterile glass window fixed in place using tissue adhesive. Implanted animals were transferred to the intravital imaging system (Nikon, Melville, NY) for baseline measurement and later reanesthetized for additional imaging with MetaMorph Imaging software (Universal Imaging, Downingtown, PA). Measurements were restricted to a fixed region within each image throughout the course of the study.

Affymetrix GeneChip analysis. CGNPs were isolated from Percoll density gradients. Tumors were collected, flash frozen, and stored at −80°C. Total RNA was extracted using Trizol (Invitrogen) according to the manufacturer's instructions. RNA was subjected to microarray hybridization (19) to the GeneChip Mouse Expression Set (MOE) 430A and 430B (Affymetrix, Santa Clara, CA), which contains 45,000 probe sets representing >39,000 transcripts, including >34,000 mouse genes on two arrays. Signals were detected using Affymetrix scanners, and the expression value for each was calculated using Affymetrix MAS5 software. Affymetrix CEL files were normalized with the gcRMA model (Bioconductor 1.8), and only probes that were present in at least one of the sample groups were used. To identify genes that were differentially expressed among CGNPs and medulloblastomas, supervised analyses were carried out (20). ANOVA was applied to, and the nominal *P* value was corrected for, multiple tests with controls for the family-wise error rate. Genes were considered to be differentially expressed if the adjusted *P* value was <0.01.

Quantitative real-time PCR. Quantitative real-time PCR (Q-PCR) on RNA extracted from purified CGNP-like tumor cells was done as described (13), and data were analyzed with SDS version 2.0 software (ABI, Branchburg, NJ) normalized to the internal 18S rRNA level (19).

Results

***Ink4c* inactivation promotes anaplastic medulloblastoma.** Because *p53*-null mice develop a spectrum of tumors that greatly

[6] http://www.bioconductor.org
[7] http://genome.ucsc.edu

shorten their life span, we generated heterozygous mice containing one "floxed" (FL) and one null *p53* allele ($p53^{FL/-}$) on a transgenic background, in which Cre recombinase is expressed under the control of the *Nestin* promoter. This procedure generated animals specifically lacking *p53* in portions of the central nervous system, including CGNPs within the EGL.

Exposure of a small cohort of such animals to 4 Gy ionizing radiation at P5-P7 yielded medulloblastomas in two of five treated $Ink4c^{+/+}$ mice, whereas four of four developed medulloblastoma on an *Ink4c*-null background (13). Because the initial numbers of mice in these groups were small, we generated larger cohorts in an attempt to more precisely determine the effects of *Ink4c* loss on medulloblastoma formation. In addition, tumors arising in these animals were further analyzed for specific chromosomal aberrations associated with tumor formation. Mice were irradiated at P7 and sacrificed when moribund (Fig. 1). Those that did not show signs of disease were sacrificed and necropsied at 6 months of age. Although brain tumors were induced with similar time of onset regardless of *Ink4c* genotype, mice lacking *Ink4c* alleles succumbed more readily to medulloblastoma (*P* values in Fig. 1). Histologic analysis revealed that the frequency of the anaplastic form of medulloblastoma was increased in animals lacking one or both *Ink4c* alleles (Supplementary Table S1). Thus, in this medulloblastoma model, *Ink4c* modulates disease pathogenesis but not tumor incidence.

Genetic alterations in medulloblastomas arising in irradiated $p53^{FL/-}$, $Nestin\text{-}Cre^{+}$ mice lacking *Ink4c* alleles. Karyotypic analysis of nine such tumors revealed that the most common event in all medulloblastomas was loss of chromosome 13, either involving the elimination of an entire chromosome, loss of a fragment, or nonreciprocal translocations of a portion of chromosome 13 with other chromosomes, including chromosomes 6, 11, 12, and 9 (Table 1). In several cases, these events were confirmed by CGH analyses (examples in Supplementary Fig. 1*A* and *B*). Because *Ptc1* resides on chromosome 13, and its loss independently predisposes to medulloblastoma development (21), which is greatly accelerated on a *p53*-null background (22), further studies were undertaken to determine the status of this gene in these and additional medulloblastoma cases.

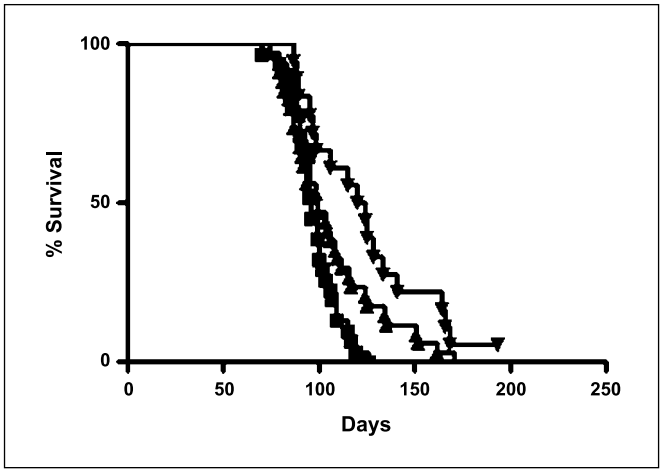

Figure 1. Survival curves of irradiated $p53^{FL/-}$, $Nestin\text{-}Cre^{+}$ mice with various *Ink4c* genotypes. Number of mice in each $p53^{FL/-}$, $Nestin\text{-}Cre^{+}$ group included $Ink4c^{+/+}$ (▼, $n = 18$), $Ink4c^{+/-}$ (▲, $n = 34$), and $Ink4c^{-/-}$ (■, $n = 31$). $Ink4c^{-/-}$ versus $Ink4c^{+/+}$, $P = 0.0002$; $Ink4c^{-/-}$ versus $Ink4c^{+/-}$, $P = 0.069$; $Ink4c^{+/-}$ versus $Ink4c^{+/+}$, $P = 0.047$.

Twenty-three medulloblastomas arising in irradiated $p53^{FL/-}$, $Nestin\text{-}Cre^{+}$ mice of various *Ink4c* genotypes were analyzed by FISH using a BAC clone containing the *Ptc1* gene (Table 2). Eight tumors exhibited complete loss of *Ptc1*, 13 retained only a single copy, and 2 showed no evidence of *Ptc1* deletion. CGNP-like tumor cells from seven medulloblastomas were purified on two-step Percoll gradients, and RNAs extracted from them were examined using Q-PCR with primers that detect *Ptc1, Ink4c*, and *Math1* (the latter being highly enriched in CGNPs; ref. 13). We detected no *Ptc1* transcripts in five of five representative tumors that had lost only one copy of chromosome 13 (Table 2). Similarly, no *Ptc1* signal was generated from one of two tumors (no. 50910 in Table 2) that retained both copies of chromosome 13. In marked contrast, *Ink4c* mRNA and protein were expressed in six of six tumors that retained one *Ink4c* allele, confirming that *Ink4c*, unlike *Ptc1*, is haploinsufficient for tumor suppression (13, 23). Thus, tumors initiated in irradiated *p53*-null progenitor cells that lack one or two *Ink4c* alleles routinely inactivate *Ptc1* in the course of tumor development.

The next most frequent genetic alteration detected in these medulloblastomas involved chromosome 6 (Table 1). Of nine medulloblastomas analyzed, trisomy 6 was found in three (Supplementary Fig. 1*C*), ins(6;2) in one of nine, and a nonreciprocal translocation with chromosome 2 in one of nine medulloblastomas. Most tumors acquired a gain of chromosome 6 or part of it, although we found one (tumor 47966) that lost an intact chromosome 6 but instead exhibited a derivative containing portions of this chromosome (Tables 1 and 2). Aberrations involving chromosome 6 were also observed in tumors independently arising in mice lacking *Ptc1* and *Ink4c* but retaining wild-type (WT) *p53* (see below), suggesting that such anomalies are characteristic of medulloblastomas arising in cells containing different predisposing genetic lesions.

In these nine tumors, we also observed rearrangements or gain of chromosome 12 in four, loss of chromosome 19 in three (Supplementary Fig. 1*D*), and loss of chromosome 7 in two (Table 1). Other chromosomal alterations were not consistently found. Although *Pten* maps to chromosome 19, we observed no increase in phospho-Akt in tumors lacking this chromosome (data not shown). SKY analysis revealed an amplification of a portion of chromosome 12 in the form of double minutes in two of these tumors, as confirmed by CGH analysis (Table 1; Supplementary Fig. 1*E*). FISH and CGH confirmed that N-*Myc* was amplified in these tumors (Supplementary Fig. 1*E*). Array CGH also revealed an amplicon on chromosome 7 that encodes cyclin D1, and FISH detected increased *cyclin D1* copy numbers in 9 of 10 medulloblastomas so analyzed (tumor numbers indicated in footnote in Table 2; Supplementary Fig. 1*F*).

Increases in N-*Myc* and *Ccnd1* copy numbers detected in medulloblastoma samples or in CGNP-like tumor cells purified from them correlated with augmented levels of expression of the respective proteins (Fig. 2*B* and *C*). For example, tumor 47966 (Fig. 2*B*) and tumor 50863 (Fig. 2*C*), which contained double minutes and exhibited N-*Myc* amplification (Tables 1 and 2), expressed the highest levels of the N-Myc protein of all tumors analyzed. Similarly, tumors 49743 (Fig. 2*B*) and 51097 (Fig. 2*C*), in which two or four copies of *Ccnd1* were detected by FISH (Table 2), expressed the highest levels of cyclin D1 protein. Like the patterns of protein expression in normal P5 cerebellum (Fig. 2*A, left lane*), the levels of expression of cyclin D2 eclipsed those of cyclin D1 in these tumor cells, whereas no tumor-specific alterations were

Table 1. Recurrent chromosomal aberrations in medulloblastomas arising in irradiated *p53*$^{FL/-}$, *Nestin-Cre*$^{+}$ mice of different *Ink4c* genotypes

Tumor no.	*Ink4c* genotype	Chromosome 13 (no. indicated events/ no. metaphases)	Chromosome 6 (no. indicated events/ no. metaphases)	Others (no. indicated events/ no. metaphases)
49739	+/+	−13 (5/11) der(13)t(12;13) (4/11) del(13) (2/11)	+6 (3/11)	−X/Y (11/11) del(8) (8/11) 11 [der(11)t(8;11) (2/11); ins(11;8) (6/11); der(11) (3/11)] dmin(12)(5/11) with N-*Myc* amp −19 (4/11)
43726	+/−	−13 (2/9) der13t(6;13) (7/9)	der(6)t(2;6) (4/9) der(6)t(2;6;?) (2/9) ins(6;2)(1/9) der(14)t(6;14) (9/9)	−Y (5/9) der(2)t(2;X, 3, 5, 8, or 16) (8/9)
43512	+/−	−13 (12/12)	None	der(3)t(3;2 or 11) (12/12) −7 (12/12) der(8)(t8;16) (12/12) der(11)t(11;3, 8, or 16) (12/12) del(14) (12/12) del(15) (12/12) −16 (12/12)
48819	+/−	−13 (12/12)	+6 (12/12)	+Y (12/12) +4 (12/12) +5 (12/12) ?der(15)t(15:?) (12/12) +17 +17+17 (12/12) +18 (12/12) *Ccnd1* (4 copies)
52160	+/−	−13 (10/10)	None	12 [+12 (1/10); dup(12) (6/10); t(7;12) dup(12) (1/10)]
52535	+/−	der(13)t(11;13) (8/8)	der(X)t(X;6) (2/8) der(11)t(6;11) (2/8)	11[der(11)t(?X;11) (1/8); der(11)t(7;11) (1/8);del(11) (1/8); der(11)t(11;?14) (1/8)]
40104	−/−	−13 (9/10); der(13)t(9;13) (1/10)	+6 (10/10) der(7)t(6;7) (1/10)	7[−7 (2/10); del(7) (1/10)]; −16 (4/10) −19 (7/10)
47966	−/−	der(13)t(6;13) (9/9)	−6 (9/9) der(18)t(6;18) (9/9)	cf(11;17) (9/9) 12 [der(12)t(12;18) (1/9); −12 (4/9); der(12)t(1;12) (1/9); del(12) (1/9) dmin(12) (5/9) with N-*Myc* amp] −19 (9/9)
53072	−/−	−13 (6/11) del(13) (5/11)	None	del(12) (6/11) del(16) (11/11)

Abbreviations: del, deletion; der, derivative; cf, centric fusion; dmin, double minute; ins, insertion; t, translocation; dup, duplication; amp, amplification.

observed in Cdk4 and Cdk2 (Fig. 2*B* and *C*). Based on these data, we designed additional experiments to explore the potential roles of cyclin D1 and N-Myc overexpression in the context of medulloblastoma development (see below).

Trisomy 6 also occurs in medulloblastomas arising in *Ptc1*$^{+/-}$ mice lacking *Ink4c*. *Ink4c* loss also increases the incidence of medulloblastoma development in *Ptc1*$^{+/-}$ mice, but in this setting, p53 function is retained (13). Thus, *Ink4c* and *p53* can collaborate independently with *Ptc1* to initiate disease. In contrast to the complex genotypic changes observed in medulloblastomas lacking *p53* and *Ink4c* (Table 1), tumors arising in *Ptc1*$^{+/-}$ mice, whether lacking *Ink4c* alleles or not, did not display complex karyotypic alterations (Table 3). Most such tumors were diploid and contained 40 to 41 chromosomes, implying that, as expected, retention of p53 helps to preserve genomic stability. SKY or CGH analysis revealed that none of these tumors lost chromosome 13, and FISH analysis did not detect deletions of the remaining WT *Ptc1* allele in six medulloblastomas analyzed in this manner. Nonetheless, Q-PCR of purified CGNP-like tumor cells showed that *Ptc1* RNA was not detectably expressed in any of these tumors, whereas *Ink4c* expression was retained in those medulloblastomas that arose in *Ink4c*$^{+/-}$ mice, again arguing that, in this medulloblastoma model as well, there is a strong selection for complete inactivation of *Ptc1* function but not for *Ink4c* (13).

Interestingly, 5 of 11 medulloblastomas arising in *Ptc1*$^{+/-}$, *Ink4c*$^{+/-}$ or in *Ptc1*$^{+/-}$, *Ink4c*$^{-/-}$ mice also acquired an extra chromosome 6 (Table 3), similar to what was observed in medulloblastomas arising in mice lacking both *Ink4c* and *p53*

(Table 1). Therefore, regardless of whether p53 function was retained or lost, trisomy of chromosome 6 was associated with inactivation of *Ptc1* and loss of one or two *Ink4c* alleles.

Distinctive clinicopathologic and molecular features of the two medulloblastoma models. Medulloblastomas initiated in irradiated *p53*-null progenitors tended to be much more invasive than those that retained p53 function. Tumors arising in *Ink4c*$^{+/-}$, *p53*$^{FL/-}$, *Nestin-Cre*$^{+}$ mice were found in the molecular layer but invaded inward toward the IGL and the brain stem (Supplementary Fig. 2*A* and *B*), whereas those arising in *Ptc1*$^{+/-}$, *Ink4c*$^{-/-}$ (or *Ink4c*$^{+/-}$) mice were generally restricted to the periphery of the cerebellum (Supplementary Fig. 2*C* and *D*). Consequently, mice with the latter medulloblastomas followed a more indolent clinical course, such that when they developed overt signs of disease, they frequently had massive tumors but ones that were more confined to the cerebellum.

With the exception of tumors, in which N-*Myc* was amplified on double-minute chromosomes (Fig. 2, tumors 47966 and 50863), comparison of expression of several targets of the Shh signaling pathway by immunoblotting showed that the levels of expression of the N-Myc, cyclin D2, Cdk4, and Cdk2 proteins were generally similar in both classes of medulloblastoma (compare Fig. 2*D* and *B*). This fits with the idea that *Ptc1* was inactivated regardless of the initiating genetic lesions. In contrast, cyclin D1 and Cdk6 were more highly expressed in tumors arising in *Ptc1*$^{+/-}$ mice that retained p53 (Fig. 2*D*) when compared with their levels of expression in normal P5 cerebellum (Fig. 2*A, left lane*) or in tumors arising in *p53*-null cells (Fig. 2*B* and *C*). However, FISH and CGH failed to reveal additional copies of cyclin D1 in the tumors arising in *Ptc1*$^{+/-}$ mice, implying that increases in gene copy number did not account for the significant increase in cyclin D1 expression in this setting.

Generation of tumors from primary CGNPs. Because amplification of N-*Myc* and increased *Ccnd1* copy number occurred in a subset of tumors that arose in irradiated *p53*$^{FL/-}$, *Nestin-Cre*$^{+}$ mice (Tables 1 and 2), we tested whether enforced expression of N-*Myc* or *cyclin D1* in primary CGNPs purified from *Ink4c*$^{-/-}$, *p53*$^{-/-}$ tumor-prone mice could induce medulloblastoma formation. Purified CGNPs from P6 mice lacking both of these genes were infected with high titer retroviruses expressing GFP, without or together with N-*Myc* or *Ccnd1/cyclin D1*. CGNPs infected with a control vector expressing GFP alone failed to proliferate in culture in the absence of Shh and did not incorporate bromodeoxyuridine. In contrast, infection of *Ink4c, p53* doubly deficient CGNPs with retroviruses encoding N-Myc or cyclin D1 stimulated them to divide under the same culture conditions (data not shown).

We then injected 2×10^6 infected CGNPs into the cerebral cortex of recipient immunocompromised mice. A glass window was surgically placed over the injected area, thereby enabling us to monitor the proliferation of GFP-marked cells and to follow any tumor development in live animals in real time by use of intravital fluorescence microscopy. Medulloblastomas did not develop when

Table 2. FISH and SKY analysis of *Ptc1* in medulloblastomas arising in irradiated *p53*$^{FL/-}$, *Nestin-Cre*$^{+}$ mice of different *Ink4c* genotypes

Tumor no.	*Ink4c* genotype	FISH (*Ptc1* deletion)	SKY (chromosome 13)*	Q-RT-PCR† (*Ptc1/Ink4c/Math1*)
49739	+/+	Homozygous	−13 (5/11); del(13)(2/11); der(13)t(12;13) (4/11)	
50861	+/+	Homozygous		
50912	+/+	Hemizygous		
43512	+/−	Homozygous	−13	
48819‡	+/−	Hemizygous	−13	
48821‡	+/−	Hemizygous		(−/+/+)
49740	+/−	Hemizygous		
49741	+/−	Hemizygous		
49743‡	+/−	Homozygous		
50863‡,§	+/−	Hemizygous	Normal	(−/+/+)
50885‡	+/−	Homozygous	der(13)t(3;13)	(−/+/+)
50903	+/−	Hemizygous		
50904‡	+/−	Hemizygous		(−/+/+)
50910‡	+/−	None		(−/+/+)
51089‡	+/−	Hemizygous	−13	(−/+/+)
52160	+/−	Homozygous	−13	
52163	+/−	Homozygous		
52532	+/−	None		
52535	+/−	Hemizygous	der13 t(11;13)	
47966§,‖	−/−	Hemizygous	der13 t(6;13)	
51087	−/−	Homozygous		
51097‡	−/−	Hemizygous	−13 (2/7); del(13) (4/7); t(X;13) (7/7)	(−/−/+)
52542	−/−	Hemizygous		

*(no. indicated events/no. metaphases).
†RNA isolated from purified tumor cells was analyzed by quantitative Q-PCR for *Ptc1, Ink4c*, and *Math1* expression.
‡FISH analysis revealed increased copies (2-3 or 2-4) of *Ccnd1* per cell.
§FISH analysis revealed amplification of *N-Myc*.
‖FISH analysis revealed normal copies (2) of *Ccnd1* per cell.

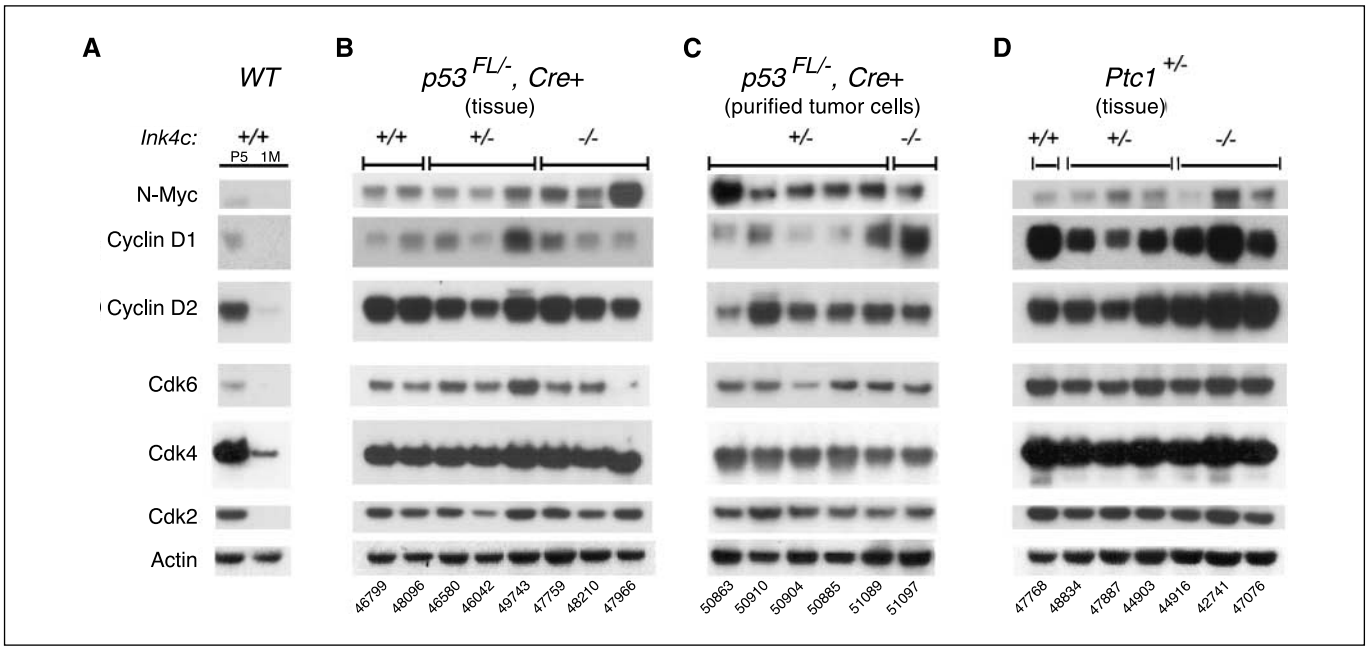

Figure 2. Protein expression in medulloblastomas initiated in mice of different genotypes. Proteins were extracted from the cerebellum of WT mice at P5 and 1 mo (*1M*) of age (*A*), from medulloblastoma tissues (*B* and *D*), or from CGNP-like tumor cells purified on Percoll gradients (*C*). The different initiating mutations predisposing to medulloblastoma development are noted at the top of (*B–D*), with their *Ink4c* genotypes denoted below. Proteins (*left*) were detected by immunoblotting. All $p53^{FL/-}$, *Nestin-Cre*$^{+}$ mice (*B* and *C*) were irradiated at P7. Tumor numbers discussed in the text are indicated below the lanes. Tumors 47966 and 50863 exhibited *N-Myc* amplification revealed by FISH and SKY.

Ink4c/p53 doubly null cells infected with a control GFP vector were injected into the brain (none of three mice). However, cells infected with vectors encoding either N-Myc (four of six mice) or cyclin D1 (two of five mice) generated medulloblastomas. Foci of green fluorescent cells were detected as early as 1 week after injection, and tumors necessitating sacrifice of the animals arose from 8 to 32 weeks after injection (Fig. 3*A*). Excised tumors analyzed histopathologically had typical characteristics of medulloblastomas, as indicated by the size and morphology of tumor cells as well as by expression of neuronal and glial markers (Fig. 3*B*). Enforced cyclin D1 and GFP expression was confirmed by immunostaining of tumor sections with their respective antibodies (Fig. 3*B*). Antibodies to N-Myc were unable to detect protein expression by immunohistochemistry, and thus, in these tumors, only GFP expression was monitored.

Using Affymetrix GeneChip analysis, we compared the gene expression profiles of the orthotopically arising medulloblastomas with those arising spontaneously in $Ink4c^{-/-}$, $p53^{-/-}$ mice (Fig. 3*Ca*, compare *lanes 1* and *2* versus *lanes 3–5*, respectively), as well as with expression profiles generated with CGNPs purified from WT P6 pups (Fig. 3*C, lanes 6–8*) and P5 whole cerebellum (Fig. 3*C, a lanes 9–11*). All medulloblastomas were found to share similar patterns of gene expression with profiles closer to those of purified CGNPs from P5 mice than from whole P5 cerebellum.

Table 3. Genetic anomalies in medulloblastomas arising in $Ptc^{+/-}$ mice lacking *Ink4c* alleles

Tumor no.	*Ink4c* Genotype	Karyotype, SKY (no. indicated events/ no. metaphases)	CGH	FISH, *Ptc1* deletion
50058	+/+	Normal	Normal	None
33094	+/−	+6 (4/6)	ND	ND
38829	+/−	+6 (9/9)	ND	ND
42864	+/−	Normal	ND	ND
47887	+/−	+14 (9/9)	+14	None
48834	+/−	ND	Normal	ND
50783	+/−	−X/Y (4/4) +6 (4/4)	−X	None
51045	+/−	ND	+X	None
42741	−/−	ND	+6	None
44916	−/−	ND	+6	ND
48195	−/−	ND	Normal	None

Abbreviation: ND, not done.

Chromosomal cytoband analysis revealed complete loss of expression of all the genes encoded by chromosome 13 represented on the array (data not shown) confirming SKY and CGH analysis of the spontaneous tumors. Together, these experiments affirm that CGNPs are target cells for medulloblastoma formation and show that N-Myc and cyclin D1 overexpression, two common events seen in human medulloblastomas, collaborate with mutations in *Ptc1, Ink4c*, and, in some cases, *p53* to induce medulloblastomas in mice.

Discussion

Role of p53 in mouse medulloblastoma. The cerebellum is particularly sensitive to DNA damage during postnatal organogenesis. This has been amply shown in different mouse models of medulloblastoma, in which genes that regulate DNA damage signaling and repair (e.g., *Ligase4, Parp-1*, and *Xrcc4*) were deleted together with *p53* (24–26). Irradiation of *p53*-null mice at P7 induces medulloblastomas whose aggressive nature is augmented by concomitant inactivation of *Ink4c*. Karyotypic and SKY analyses of these tumors revealed complex chromosomal rearrangements, including losses and gains, as well as translocations, deletions, insertions, and duplications. In contrast, medulloblastomas arising in $Ptc1^{+/-}$ mice lacking one or two *Ink4c* alleles retain p53 function (13) and harbor fewer chromosomal rearrangements, implying that many of the genetic anomalies observed in the irradiated *p53*-null animals are a consequence of genomic instability but are unlikely to initiate medulloblastoma formation (27).

Medulloblastomas lacking *p53* and *Ink4c* were more anaplastic and invasive than those initiated in mice lacking one copy of *Ptc1* and *Ink4c*. We noted that tumors occurring in *Ink4c, p53*-double

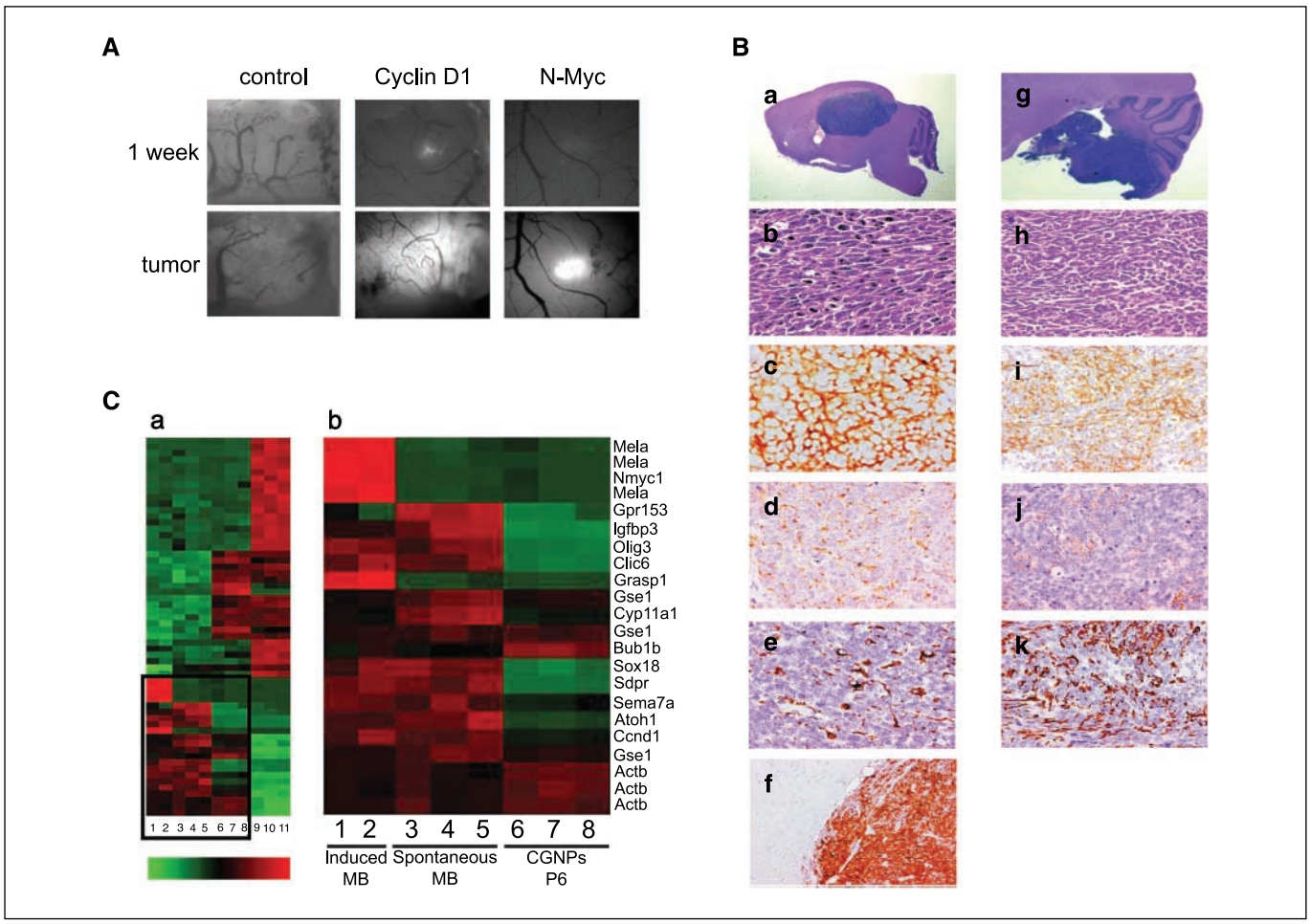

Figure 3. Enforced expression of N-Myc and cyclin D1 in P5 CGNPs from $p53^{-/-}$, $Ink4c^{-/-}$ mice induces medulloblastoma after orthotopic transplantation into the cerebral cortex. *A, in vivo* fluorescence imaging of tumor development from infected CGNPs implanted into the brains of immunocompromised CD-1 *nu/nu* recipient mice. Purified CGNPs from $Ink4c^{-/-}$, $p53^{-/-}$ mice were infected with retroviral vectors expressing cyclin D1 or N-Myc together with GFP or with a control virus expressing GFP alone (*top*). *B,* histopathology of brain tumors arising after injection of *Ink4c, p53* doubly deficient CGNPs overexpressing N-Myc (*a–f*) compared with that in tumors arising in irradiated $Ink4c^{-/-}$, $p53^{FL/-}$, *Nestin-Cre*$^{+}$ mice (*g–k*). *a,* H&E staining of tumor tissue developing from cells injected into the cerebral cortex versus that of a cerebellar tumor arising in an irradiated $Ink4c^{-/-}$, $p53^{FL/-}$, *Nestin-Cre*$^{+}$ mouse (*g*). *b* and *h,* H&E staining (magnification, ×400) showing the typical morphology of medulloblastoma cells. *c* and *i,* tumor cells stained strongly for class III β-tubulin (TUJ1; magnification, ×400) and showed diffuse expression of synaptophysin (magnification, ×400) (*d* and *j*), both of which are neuronal markers. *e* and *k,* like human medulloblastomas, many mouse tumors showed glial differentiation as evidenced by sporadic GFAP expression (magnification, ×400). *f,* tumor cells stained positively for GFP (magnification, ×400) as opposed to adjacent normal tissue that did not. *C,* microarray analysis of medulloblastomas arising orthotopically (*lanes 1* and *2*) and spontaneously (*lanes 3–5*) and of CGNPs from WT P6 pups (*lanes 6–8*) and P5 total cerebellum (*lanes 9–11*). Microarray data were subjected to ANOVA and genes that changed >1.9-fold between the indicated groups (with adjusted *P* values <0.01 and maximum absolute intensity difference >32 units) were considered differentially expressed (*a*). Colors represent relative expression level. *Red,* high expression; *green,* low expression (see gradient). Genes were clustered based on expression pattern among the four groups. *b,* an expanded view of the boxed area in (*a*) that contains genes overexpressed in medulloblastoma samples. The individual gene names (*right*) correspond to the denoted rows in the cluster.

null or in irradiated $p53^{FL/-}$, *Nestin-Cre*$^+$ mice were located within the EGL but invaded inward into the IGL and toward the brain stem. In contrast, medulloblastomas arising in $Ptc1^{+/-}$, *Ink4c*-null mice arose in the cerebellar periphery and did not invade the IGL. Because the latter tumors were more restricted in position and less anaplastic, they tended to become very large before clinical signs of disease were overt. Therefore, we suspect that the relatively increased genetic instability of *p53*-null medulloblastomas, although not strictly responsible for tumor initiation, likely contributes to tumor anaplasia and to increased invasive properties. In addition, although infrequent, *TP53* mutations in human medulloblastomas are associated with large cell anaplastic features (8) that are recapitulated in the $Ink4c^{-/-}$, $p53^{-/-}$ mouse medulloblastoma model.

***Ptc1* inactivation.** Although medulloblastomas initiated in the $Ink4c^{-/-}$, $p53^{-/-}$ and $Ink4c^{-/-}$, $Ptc1^{+/-}$ backgrounds exhibited karyotypes with different complexities, they shared specific genetic alterations. Remarkably, the most common event seen in spontaneously arising medulloblastomas lacking *p53* with or without inactivation of *Ink4c* was the loss of one chromosome 13 or its translocation with other chromosomes, leading to hemizygous or homozygous loss of the *Ptc1* gene. Complete loss of *Ptc1* expression was evident in all medulloblastomas examined regardless of whether chromosome 13 was retained. Orthotopically derived tumors lacking *p53* and *Ink4c* also loose chromosome 13 and *Ptc1* function and similarly yield expression profiles that show activation of the Shh signaling pathway. Frequent loss of one chromosome 13 was also observed in two other mouse models that stemmed from conditional loss of *p53* together with *Rb* or *Xrcc4*, respectively (26, 27). These results support the idea that, at least in mice, loss of genomic stability, together with loss of normal DNA repair or of a functional retinoblastoma pathway, are themselves insufficient to induce medulloblastomas and require *Ptc1* inactivation.

Although genetic analyses of mouse medulloblastomas arising either spontaneously or "engineered" from primary CGNPs suggest that their development can be triggered by many of the same genetic alterations found in human medulloblastomas, the uniform involvement of *Ptc1* was unexpected given that only ~25% human medulloblastomas show activation of the Shh signaling pathway (3, 6). A survey of mutations in a cohort of 46 human medulloblastomas revealed mutually exclusive activation of the Shh/Ptc versus the Wnt/β-catenin signaling pathways with an overall incidence of ~20% for each (6). This underscores the present inadequacy of mouse models in mimicking certain forms of human medulloblastoma and raises the issue of whether it will be possible to derive mouse models of human medulloblastoma, in which *Ptc1* function is preserved.

Other recurrent genetic lesions. The next most common genetic event observed in medulloblastomas arising in both of our mouse models involved chromosome 6, as manifested by the gain of a whole chromosome leading to trisomy 6 or by translocations with other chromosomes. Trisomy 6 is also a frequent event in mice, in which *Xrcc4* and *p53* are targeted to the central nervous system (CNS; ref. 26). The genes encoding cyclin D2, cyclin E, and Fox M1 are located on this chromosome and are attractive potential candidates in contributing to tumor formation. However, the *cyclin D2* gene is a direct target of the Shh/Ptc signaling pathway and is expressed at relatively high levels in the Shh-driven development of the postnatal cerebellum (28) and was therefore expected to be highly expressed in tumors, in which the pathway is constitutively activated by *Ptc1* loss. Indeed, immunoblotting revealed robust expression of this protein in all tumors from *Ink4c*-compromised $Ptc1^{+/-}$ or $p53^{FL/-}$, *Nestin-Cre*$^+$ mice whether they exhibited a gain of chromosome 6 or not. FISH analysis of several translocations failed to reveal common breakpoints on chromosome 6 providing no clue to the identity of the target gene(s).

Other chromosomal gains or losses were less frequent. Interestingly, three of nine $p53^{FL/-}$, *Nestin-Cre*$^+$ medulloblastomas exhibited monosomy 19. Loss of one chromosome 19 was also a frequent event (four of eight tumors analyzed) in $Rb^{FL/-}$, $p53^{FL/-}$, *Nestin-Cre*$^+$ medulloblastomas (27). Notably, two tumor suppressors, *Pten* and *Sufu*, map to mouse chromosome 19, but we saw no correlation between the loss of chromosome 19 and levels of phospho-Akt. Moreover, *Pten* mutations are exceedingly rare in human medulloblastomas.

In $p53^{FL/-}$, *Nestin-Cre*$^+$ medulloblastomas lacking *Ink4c* alleles, we found that several tumors exhibited three to four copies of *Ccnd1*, only two of which exhibited elevated cyclin D1 protein levels. Several of these tumors lacked one copy of chromosome 7 on which *Ccnd1* is located, providing a possible explanation for variations in cyclin D1 expression. Strikingly, cyclin D1 protein levels were high in all medulloblastomas arising in $Ptc1^{+/-}$ mice regardless of *Ink4c* status, but its high expression did not result from gene amplification, increased copy number, or chromosomal translocations.

We observed two medulloblastomas, in which N-*Myc* located on chromosome 12 was amplified on double-minute chromosomes and was highly expressed. N-*Myc* amplification has been observed in 5% of human medulloblastomas and is associated with the large cell/anaplastic subtype. However, overexpression of N-*Myc* unaccompanied by amplification occurs in 55% to 88% of such tumors (5, 29, 30). N-*Myc* is also a direct target of the Shh signaling pathway (31) and is required for proliferation of CGNPs during cerebellar development. Its conditional deletion early in CNS development leads to cerebellar microcephaly and to severe cerebellar developmental defects (32). N-*Myc* amplification was also a common event in medulloblastomas arising in other mouse models (26, 27). Although cyclin D1 is regulated by N-Myc (28, 33), we saw no correlation between high levels of N-Myc and those of cyclin D1.

Enforced expression of cyclin D1 and N-Myc in CGNPs from tumor-prone mice induces medulloblastomas. To test whether amplification or overexpression of cyclin D1 or N-Myc were important for tumor formation, we introduced them by retroviral gene transfer into purified CGNPs from genetically engineered mice lacking *p53* and *Ink4c* and injected the modified CGNPs into the cortex of recipient mice under cranial windows. Not only did these genes provide CGNPs with a proliferative advantage *in vitro*, as shown also by others (33), but they also contributed to tumor formation *in vivo*. Marking the cells with GFP enabled us to follow cell proliferation and tumor formation in live animals in real time, thus providing a powerful method to test the contribution of candidate genes to medulloblastoma development.

Analysis of these orthotopically induced medulloblastomas by Affymetrix GeneChip Microarrays revealed that they shared similar gene expression profiles with tumors spontaneously arising in tumor prone mice. This again implies that many of the complex chromosomal translocations and alterations seen in tumors arising in irradiated $p53^{FL/-}$, *Nestin-Cre*$^+$ mice, with or without the loss of *Ink4c* alleles, has little bearing on tumor initiation. Inactivation of N-*Myc* or *cyclin D1* not only impairs cerebellar development but also suppresses medulloblastoma formation in mouse models where the

Shh pathway is activated (34, 35), underscoring the role of these two oncogenes in medulloblastoma development. Conversely, these results emphasize how defined combinations of oncogenes and tumor suppressors interact to initiate full-blown medulloblastomas from primary CGNPs.

Acknowledgments

Received 9/20/2006; revised 12/13/2006; accepted 1/8/2007.

Grant support: NIH CA-96832 (M.F. Roussel), Core grant CA-21765, the Children's Brain Tumor Foundation and the Pediatric Brain Tumor Foundation (M.F. Roussel), the Emily Dorfman Foundation for Children through the American Brain Tumor Association (T. Uziel), Fondation pour la Recherche Medicale (O. Ayrault), and the American Lebanese-Syrian Associated Charities of St. Jude Children's Research Hospital. C.J. Sherr is an Investigator of the Howard Hughes Medical Institute.

The costs of publication of this article were defrayed in part by the payment of page charges. This article must therefore be hereby marked *advertisement* in accordance with 18 U.S.C. Section 1734 solely to indicate this fact.

We thank Youngsoo Lee for technical expertise in extracting tumor RNAs for Affymetrix GeneChip Microarray; Chunxu Qu and the Hartwell Center for Affymetrix GeneChip Array analysis; Michael Wang and Dianna Naeve for CGH analysis; Xiabin Yuan and Cheng Cheng for statistical analysis; Virginia Valentine for her help with SKY and FISH analysis; Dorothy Bush for immunohistochemical analysis; Robert Jenson, Shelly Wilkerson, and Deborah Yons for mouse colony management; Rose Mathew and Marie Assem for mouse genotyping; Deb Johnson and John Killmar for helping with cranial surgery; Nader Chalhoub and Suzanne Baker for providing antibodies to Pten and phospho-Akt; and all the members of the laboratory for helpful discussions.

References

1. Kleihues PC, Cavenee WK. World Health Organization Classification of Tumours: Pathology and Genetics: Tumours of the Nervous System-IARC Press; 2000. p. 129–48.
2. Gilbertson RJ. Medulloblastoma: signalling a change in treatment. Lancet Oncol 2004;5:209–18.
3. Fogarty MP, Kessler JD, Wechsler-Reya RJ. Morphing into cancer: the role of developmental signaling pathways in brain tumor formation. J Neurobiol 2005; 64:458–75.
4. Fan X, Matsui W, Khaki L, et al. Notch pathway inhibition depletes stem-like cells and blocks engraftment in embryonal brain tumors. Cancer Res 2006;66:7445–52.
5. Hallahan AR, Pritchard JI, Hansen S, et al. The SmoA1 mouse model reveals that notch signaling is critical for the growth and survival of sonic hedgehog-induced medulloblastomas. Cancer Res 2004;64:7794–800.
6. Thompson MC, Fuller C, Hogg TL, et al. Genomics identifies medulloblastoma subgroups that are enriched for specific genetic alterations. J Clin Oncol 2006;24: 1924–31.
7. Marino S. Medulloblastoma: developmental mechanisms out of control. Trends Mol Med 2005;11:17–22.
8. Frank AJ, Hernan R, Hollander A, et al. The TP53-ARF tumor suppressor pathway is frequently disrupted in large/cell anaplastic medulloblastoma. Brain Res Mol Brain Res 2004;121:137–40.
9. Wang VY, Zoghbi HY. Genetic regulation of cerebellar development. Nat Rev Neurosci 2001;2:484–91.
10. Goldowitz D, Hamre K. The cells and molecules that make a cerebellum. Trends Neurosci 1998;21:375–82.
11. Wechsler-Reya RJ, Scott MP. The developmental biology of brain tumors. Annu Rev Neurosci 2001;24:385–428.
12. Read TA, Hegedus B, Wechsler-Reya R, Gutmann DH. The neurobiology of neurooncology. Ann Neurol 2006; 60:3–11.
13. Uziel T, Zindy F, Xie S, et al. The tumor suppressors Ink4c and p53 collaborate independently with Patched to suppress medulloblastoma formation. Genes Dev 2005;19:2656–67.
14. Zindy F, Nilsson LM, Nguyen L, et al. Hemangiosarcomas, medulloblastomas, and other tumors in Ink4c/p53-null mice. Cancer Res 2003;63:5420–7.
15. Snijders AM, Nowak NJ, Huey B, et al. Mapping segmental and sequence variations among laboratory mice using BAC array CGH. Genome Res 2005;15: 302–11.
16. Nowak NJ, Snijders A, Conroy J, Albertson D. The BAC resources. Curr Protocols Hum Genet 2005;4.13: 1–31.
17. Yang YH, Dudoit S, Luu P, et al. Normalization for cDNA microarray data: a robust composite method addressing single and multiple slide systematic variation. Nucleic Acids Res 2002;30:e15.
18. Hatten ME, Gao WQ, Morrison ME, Mason CA. The cerebellum: purification and coculture of identified cell populations. In: Banker G, Goslin K, editors. Culturing nerve cells. Cambridge (MA): The MIT Press; 1998. p. 419–59.
19. Lee Y, Miller HL, Jensen P, et al. A molecular fingerprint for medulloblastoma. Cancer Res 2003;63: 5428–37.
20. Holm S. A simple sequentially rejective multiple test procedure. Scand J Stat 1979;6:65–70.
21. Goodrich LV, Milenkovic L, Higgins KM, Scott MP. Altered neural cell fates and medulloblastoma in mouse patched mutants. Science 1997;277:1109–13.
22. Wetmore C, Eberhart DE, Curran T. Loss of p53 but not ARF accelerates medulloblastoma in mice heterozygous for patched. Cancer Res 2001;61:513–6.
23. Bai F, Pei XH, Godfrey VL, Xiong Y. Haploinsufficiency of p18(INK4c) sensitizes mice to carcinogen-induced tumorigenesis. Mol Cell Biol 2003;23: 1269–77.
24. Lee Y, McKinnon PJ. DNA Ligase IV suppresses medulloblastoma formation. Cancer Res 2002;62: 6395–9.
25. Tong WM, Ohgaki H, Huang H, et al. Null mutation of DNA strand break-binding molecule poly(ADP-ribose) polymerase causes medulloblastomas in p53(−/−) mice. Am J Pathol 2003;162:343–52.
26. Yan CT, Kaushal D, Murphy M, et al. XRCC4 suppresses medulloblastomas with recurrent translocations in p53-deficient mice. Proc Natl Acad Sci U S A 2006;103:7378–83.
27. Shakhova O, Leung C, van ME, Berns A, Marino S. Lack of Rb and p53 delays cerebellar development and predisposes to large cell anaplastic medulloblastoma through amplification of N-Myc and Ptch2. Cancer Res 2006;66:5190–200.
28. Kenney AM, Rowitch DH. Sonic hedgehog promotes G(1) cyclin expression and sustained cell cycle progression in mammalian neuronal precursors. Mol Cell Biol 2000;20:9055–67.
29. Aldosari N, Bigner SH, Burger PC, et al. MYCC and MYCN oncogene amplification in medulloblastoma. A fluorescence *in situ* hybridization study on paraffin sections from the Children's Oncology Group. Arch Pathol Lab Med 2002;126:540–4.
30. Garson JA, Pemberton LF, Sheppard PW, et al. N-myc gene expression and oncoprotein characterisation in medulloblastoma. Br J Cancer 1989;59:889–94.
31. Knoepfler PS, Kenney AM. Neural precursor cycling at sonic speed: N-Myc pedals, GSK-3 brakes. Cell Cycle 2006;5:47–52.
32. Knoepfler PS, Cheng PF, Eisenman RN. N-myc is essential during neurogenesis for the rapid expansion of progenitor cell populations and the inhibition of neuronal differentiation. Genes Dev 2002;16:2699–712.
33. Oliver TG, Grasfeder LL, Carroll AL, et al. Transcriptional profiling of the Sonic hedgehog response: a critical role for N-myc in proliferation of neuronal precursors. Proc Natl Acad Sci U S A 2003; 100:7331–6.
34. Hatton BA, Knoepfler PS, Kenney AM, et al. N-myc is an essential downstream effector of Shh signaling during both normal and neoplastic cerebellar growth. Cancer Res 2006;66:8655–61.
35. Pogoriler J, Millen K, Utset M, Du W. Loss of cyclin D1 impairs cerebellar development and suppresses medulloblastoma formation. Development 2006;133: 3929–37.

Genetic Alterations in Mouse Medulloblastomas and Generation of Tumors *De novo* from Primary Cerebellar Granule Neuron Precursors

Frederique Zindy, Tamar Uziel, Olivier Ayrault, et al.

Cancer Res 2007;67:2676-2684.